



Influence of deposition temperature on structural, optical and electrical properties of sputtered Al doped ZnO thin films

A. Mosbah^{a,b,*}, M.S. Aida^a

^a Laboratoire des Couches Minces et Interfaces, Faculté des Sciences, Université Mentouri 25000 Constantine, Algeria

^b Département de Physique, Faculté des Sciences, Université Ferhat Abbas, 19000 Sétif, Algeria

ARTICLE INFO

Article history:

Received 14 August 2011

Received in revised form

19 November 2011

Accepted 24 November 2011

Available online 2 December 2011

Keywords:

ZnO

Al doping

DC sputtering

Substrate temperature

Electrical properties

Optical properties

ABSTRACT

Al doped ZnO thin films have been deposited by DC magnetron sputtering technique from ZnO–2 wt.% Al₂O₃ target onto glass and oxidized silicon substrates heated at temperature ranging between 150 and 370 °C in Ar plasma. X-ray diffraction analysis shows that the deposits have a preferential growth along the *c*-axis of the hexagonal structure. The average grain size increases from 10 to 59 nm with temperatures ranging from 150 up to 330 °C then it decreases to 45 nm at 370 °C. The root mean square (RMS) surface roughness decreases with substrate temperature from 20.9 to 4.1 nm. The films are transparent up to 90% in the visible wavelength range and the optical gap increases with substrate temperature from 3.41 to 3.64 eV. The resistivity measured in Van der Pauw configuration at room temperature is very sensitive to the substrate temperature. It decreases from 5×10^{-4} to 3×10^{-5} Ω cm when the deposition temperature increases from 150 to 370 °C. Both carrier mobility and carrier concentration were found to increase with substrate temperature.

© 2011 Elsevier B.V. All rights reserved.

1. Introduction

Currently, zinc oxide (ZnO) has received great interest owing to its wide band gap (3.3 eV), transparency, electrical and piezoelectrical properties. ZnO can be used for preparing transparent conducting contacts for solar cells, surface acoustic wave (SAW) devices and sensors [1,2]. Moreover, ZnO has increased interest in its various applications for short wavelength optoelectronics, transparent electronic materials [3–5] and tip materials of scanning probe microscopy.

Doped and undoped ZnO thin films have been extensively used in thin film solar cells owing to their higher thermal stability and good resistance to hydrogen plasma processing compared to indium tin oxide (ITO). ZnO is more useful with comparison to gallium nitride due to its larger exciton binding energy of 60 meV (25 meV for GaN) and also its abundance in both bulk and single-crystal forms [4–6].

It is known that zinc oxide has a hexagonal crystal structure. Highly textured films can be obtained when growing ZnO by numerous deposition techniques such as sol–gel [7,8], spin coating pyrolysis [9], spray pyrolysis [10], pulsed laser deposition PLD

[11], MOCVD [12], cathodic vacuum arc [13], DC and RF magnetron sputtering [14–17] and atomic layer deposition [18].

To achieve the numerous applications offered by ZnO, both high quality n and p type material are necessary. The n type doped ZnO can be obtained by doping with group III elements such as Al. The electrical and optical properties of ZnO can be improved by Al doping. Al doped ZnO (ZnO:Al) transparent conducting films show the highest conductivity among doped ZnO films [19–21]. ZnO:Al films can be prepared by sputtering using a (ZnO–Al₂O₃) composite target [22] or by the use of a co-sputtering system with ZnO and Al targets [23].

Generally sputtered thin films properties are influenced by substrate temperature, power, and pressure. The growth temperature plays a major role for thin film properties determination, the present study is focused on the influence of substrate temperature on structural, optical and electrical properties of aluminium doped zinc oxide films deposited from ZnO/Al₂O₃ composite ceramics target.

2. Experimental details

Al doped ZnO films were deposited on glass and oxidized silicon substrates using DC magnetron sputtering system from ZnO–2 wt.%Al₂O₃ target of 100 mm diameter. The substrates were thoroughly cleaned in acetone, methanol and distilled water then dried. The vacuum in the deposition chamber was driven down to 10^{-3} Pa by means of a turbo molecular pump and then the target was etched by sputtering for 15 min in argon (99.99% purity) atmosphere to clean its surface. Films deposition was made using argon plasma at 0.4 Pa pressure and DC power of 1.53 W cm^{-1} .

* Corresponding author at: Département de Physique, Faculté des Sciences, Université Ferhat Abbas 19000 Sétif, Algeria. Tel.: +213 794528663.

E-mail address: mosbah.ammam@yahoo.ca (A. Mosbah).

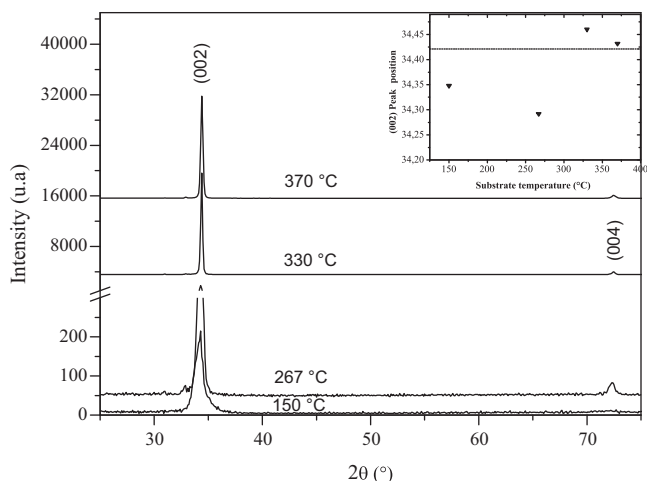


Fig. 1. XRD patterns of ZnO:Al films deposited at substrate temperature from 150 to 370 °C.

The substrate temperature was varied from 150 to 370 °C. Film structure was investigated by XRD analysis in Bragg–Brentano geometry using Cu K_{α} radiation of a Rigaku diffractometer. Film thickness was measured by profilometry using a TENCOR Alpha-Step 500 profiler. Atomic force microscopy (AFM) observations were provided by a Topometrix Explorer AFM and the roughness data were extracted using SPIP V4.2.6.0 software. The optical measurements were carried out on a Carry 500 – Varian spectrophotometer in the wavelength range from 190 to 2000 nm. Film resistivity and carrier mobility were determined at room temperature (27 °C) with Van der Pauw and Hall effect measurements, respectively.

3. Results and discussion

Sputtered ZnO thin films commonly present a hexagonal wurtzite structure. Fig. 1 shows the XRD patterns of 370 nm thick ZnO:Al films deposited at substrate temperatures ranging between 150 and 370 °C. Two diffraction peaks are recorded at 2θ angles of 34.3° and 72.3° corresponding to (002) and (004) peaks of the hexagonal wurtzite structure. As found by several authors [24,25], our deposited films have a preferential growth along c -axis direction. We also notice that the (002) peak intensity is enhanced with substrate temperature. This indicates the enhancement of the crystalline quality of ZnO:Al films. From the XRD patterns one can conclude that the incorporation of Al dopant does not affect the ZnO lattice structure by the formation of new phase since there are no observed peaks related to Al or Al_2O_3 . This result is in agreement with earlier report [26]. The preferred orientation is due to the lowest surface free energy for (002) plane [27–29]. In addition to the fact that intensity increases, we also observe that the (002) and (004) peak positions show a shift (inset Fig. 1) with respect to that of ZnO powder material $2\theta = 34.421^{\circ}$ and 72.560° , respectively presented in JCPDS (Joint Committee on Powder Diffraction Standards) File No. 36-1451. These shifts indicate the presence of a stress state in deposited films. This can be due to the incorporation of the Al as dopant in the ZnO lattice due to the different ionic radii of Al^{3+} and Zn^{2+} . However the stress is reduced at higher substrate temperatures (inset Fig. 1) which can be explained in terms of thermal relaxation.

From Fig. 2, one can notice that the full width at half maximum (FWHM) corresponding to the (002) peak decreases when substrate temperature increases up to 330 °C. Further substrate temperature increase leads to an enhancement of the FWHM. Similar results were reported by Fu et al. [30] for Al doped ZnO films studied in the substrate temperature range 50–350 °C with an increase of FWHM starting at 250 °C. The main difference between the two works is that the shift in variation tendency of FWHM is

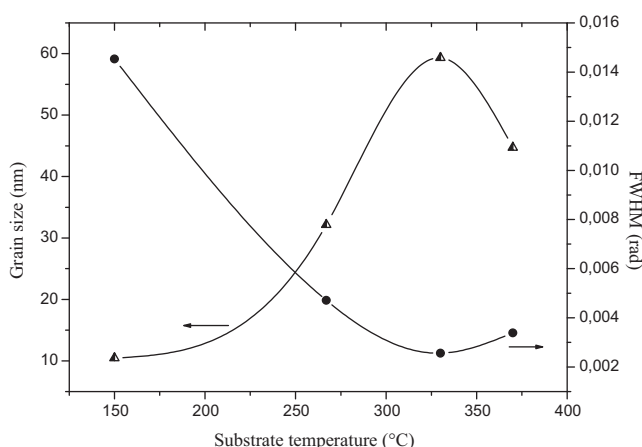


Fig. 2. Dependence of the FWHM of the (002) peak and grain size on substrate temperature for ZnO:Al films.

observed at a substrate temperature of 250 °C in [30] while in this study the tendency change is observed at 330 °C.

The average grain size G_S of the deposited films has been calculated from the FWHM of the (002) peak by using Scherrer formula [31]:

$$G_S = \frac{K\lambda}{\Delta(2\theta) \cos \theta} \quad (1)$$

where λ , θ and $\Delta(2\theta)$ are respectively, X-ray wavelength, the Bragg diffraction angle and the FWHM in radian. K is a constant that depends on crystallites shape (0.9 value is used in this work). Although this method does not take into account the strain contribution in the width of the XRD peak, it gives a good estimation of the crystallite size especially for small crystallite size [32]. The variation of the average grain size versus the substrate temperature is shown in Fig. 2. The grain size increases with substrate temperature up to 330 °C from about 10 to 59 nm. Then it decreases to 45 nm at substrate temperature of 370 °C. Similar behaviour was observed by Ma et al. [33] in DC sputtered Ga doped ZnO films in the temperature range 150–400 °C. The increase of the grain size with substrate temperature is attributed to the improvement of the ZnO:Al film crystallinity by the coalescence of small crystallites [34].

In general, surface roughness is an unavoidable property of almost all solids and so usually plays an important role in thin film physics. It was found that the substrate temperature influences the surface state of thin films. The surface morphology of ZnO:Al films grown at different substrate temperatures are revealed by atomic force microscopy. Fig. 3 shows a typical AFM image of the ZnO:Al sample deposited at 267 °C. The morphology of films exhibits a dense and compact film structure which will be effective for light-trapping in thin film silicon solar cells [35]. RMS surface roughness values of the different samples were calculated from AFM images and the obtained values are given in Table 1. These values show that the roughness of ZnO:Al films decreases with increasing growth temperature. At low temperature, the sputtered atoms reach the substrate surface with low energy, therefore their mobility is

Table 1
RMS roughness values for ZnO:Al films deposited at different substrate temperatures.

Substrate temperature (°C)	RMS roughness (nm)
150 °C	20.90
267 °C	8.81
330 °C	7.47
370 °C	4.09

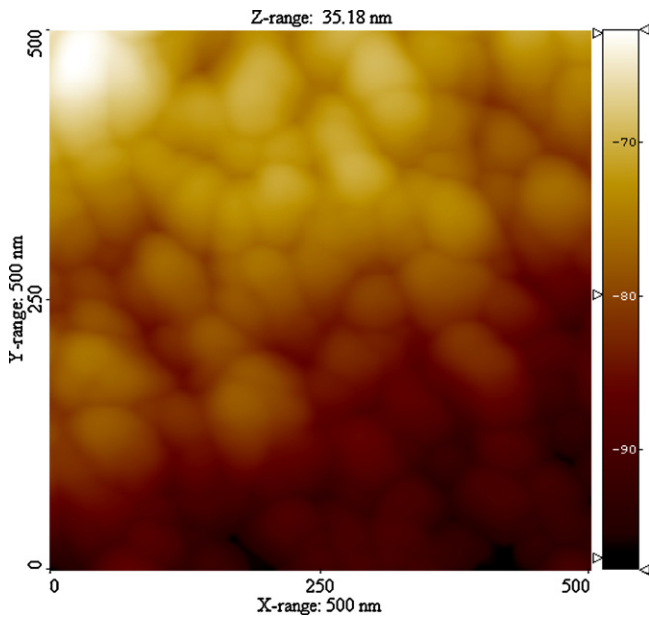


Fig. 3. AFM image of ZnO:Al film deposited at substrate temperature of 267 °C.

limited and consequently they cannot reach the appropriate sites. This explains the roughness of films deposited at low substrate temperature. With increasing substrate temperature the atoms gain enough energy and as a result their mobility on substrate surface is enhanced [36]. Thus, atoms can reach more suitable sites and this can lead to more dense and smooth films with low defects and improved crystalline quality. Comparable results were found by Ma et al. [33] in Ga doped films studied in the temperature range 150–400 °C.

The second part of this work is devoted to the study of the growth temperature influence on electrical and optical properties of ZnO:Al films.

ZnO:Al film resistivity was measured in Van der Pauw configuration at room temperature. Carrier concentration and mobility were determined by combining the electrical resistivity and Hall coefficient measurement. The resistivity variation of ZnO:Al films deposited at various substrate temperatures is displayed in Fig. 4. As can be seen, deposited films have low resistivity. The lower recorded value was $3.0 \times 10^{-5} \Omega \text{ cm}$ for the sample prepared at substrate temperature of 370 °C. Also the resistivity decreases with elevated substrate temperature. The electrical conduction in ZnO

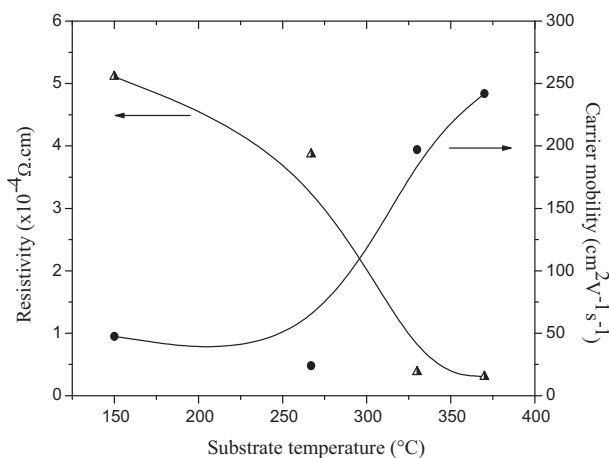


Fig. 4. Resistivity and carrier mobility versus substrate temperature for ZnO:Al films.

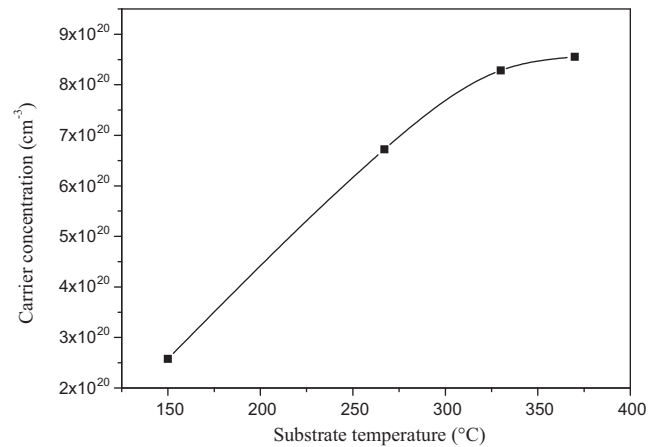


Fig. 5. Carrier concentration versus substrate temperature for ZnO:Al films.

is dominated by electrons generated from O^{2-} vacancies and Zn interstitials. However in ZnO:Al films the conductivity is better comparatively to pure ZnO films owing to Al^{3+} ions at substitutional Zn^{2+} sites [37]. The decrease of resistivity with substrate temperature is due to the enhancement of film crystallinity, carrier concentration and carrier mobility. The higher the crystal orientation the lower the resistivity. In fact, this is due to the reduction in the scattering of the carriers at the grain boundaries and crystal defects, which increases the carrier mobility as shown in Fig. 4 [19,38]. In addition, the surface roughness increases the number of oxygen traps by increasing the effective surface area. This favours the adsorption of oxygen and decreases the film conductivity which accounts for the values of resistivity recorded for the film deposited at low substrate temperature. As the substrate temperature increases, the film roughness decreases and the oxygen traps become fewer leading to the resistivity decrease. An increase of carrier concentration with substrate temperature was observed (Fig. 5) for all samples. It is clear that the electrical properties of ZnO:Al films deposited at substrate temperature of 370 °C were not affected by the decrease of grain size. This can be explained by the fact that the increase of temperature promotes the substitution of Al atoms and consequently gives more donor states. The same explanation was given to interpret the increase of carrier concentration in Ga doped ZnO with substrate temperature [33].

The transmittance spectra of deposited films are shown in Fig. 6. All films are highly transparent with a transmittance reaching the

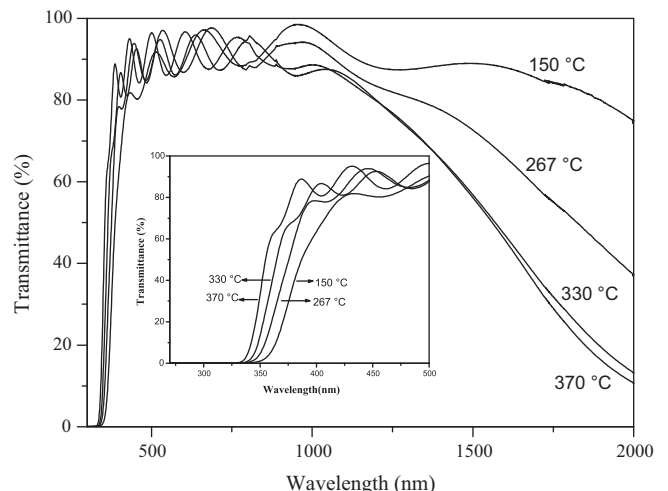


Fig. 6. Dependence of transmittance on substrate temperature for ZnO:Al films.

90% in the visible wavelength range. This is a very important result since our main goal is to prepare highly transparent and conductive electrodes for device application. In addition, the transmittance level is insensitive to the substrate temperature, even if a shift towards the higher energies of the absorption edge with increasing substrate temperature was noticed (see inset Fig. 6).

Improvement of the optical behaviour has been a predominant factor in increasing the commercial quality of opto-electronic devices. Generally transparent conducting oxides (TCO) increase light diffusion and reduce optical reflection loss [39]. These two properties are very important to obtain high collection of incident photons in solar cells. Chaabouni et al. [40] have studied the ZnO/Si structure deposited at different substrate temperatures. Their results show that the reflectance of all samples was lower than that of bare Si (30–40% in the visible range) indicating that ZnO films can be used as antireflection coatings for silicon based solar cells.

The spectra of the reflectance (R) shown in Fig. 7 confirm the low optical-reflection of ZnO:Al thin films. The reflectance is about 10% in the visible range. ZnO:Al films show an increase of the IR reflectance for wavelength higher than 1600 nm with the increase of substrate temperature in the range 150–330 °C and then slightly decreases at substrate temperature of 370 °C, this is probably due to the decrease of the grain size as shown above. The same behaviour of IR reflectance variation with substrate temperature was found by Fu et al. [30]. The decrease of IR reflectance at higher temperature was explained in terms of the change in carrier mobility.

The classic Drude model [41] correlates between the reflectance R and the vibration plasma determined by the carrier concentration N as:

$$R = 1 - 4 \left(\frac{\epsilon_0 C}{ed} \right) \times \frac{1}{N\mu} \quad (2)$$

where ϵ_0 , C , e , d and μ are respectively the permittivity of free space, light velocity, electronic charge, film thickness and carrier mobility. According to this equation, IR reflectance increases when the product $N\mu$ increases and as it was shown above, both carrier concentration and carrier mobility increase with substrate temperature. Thus, we can explain the increase of the IR reflectance with substrate temperature within the range 150–330 °C in terms of the enhancement of the product $N\mu$.

The optical band gap is calculated from the relationship between absorption coefficient and photon energy [42]:

$$\alpha hv = D(hv - E_g)^{1/2} \quad (3)$$

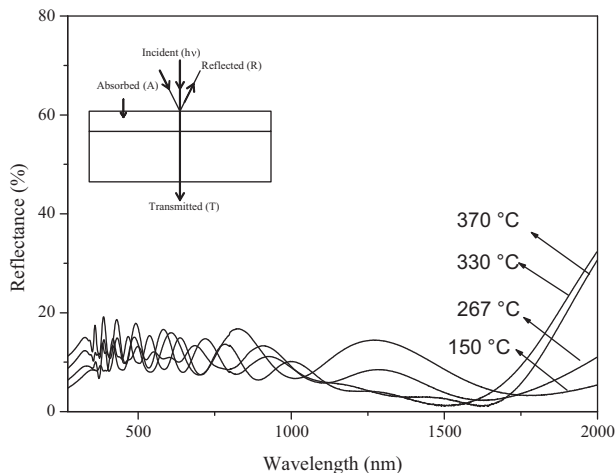


Fig. 7. Reflectance versus substrate temperature for ZnO:Al films deposited at temperatures from 150 to 370 °C.

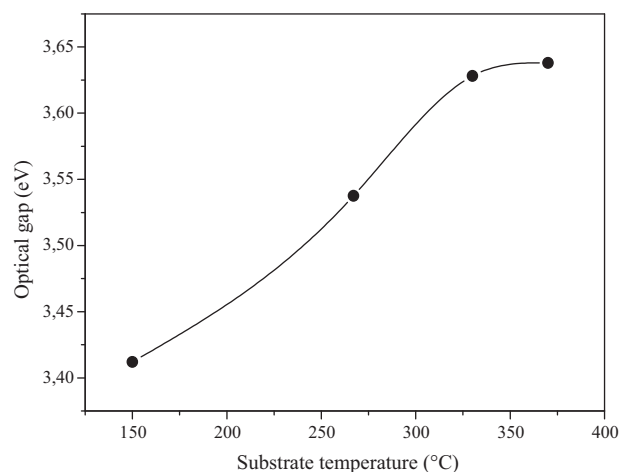


Fig. 8. Optical bandgap against substrate temperature for ZnO:Al films.

where, α is the optical absorption coefficient, $h\nu$ is the photon energy, E_g is the optical band gap, and D is a constant. E_g values are determined from the intercept of extrapolated linear portion of $(\alpha h\nu)^2$ versus $h\nu$ curve to the photon energy axis.

The absorption coefficient is calculated from the transmission spectra using the formula:

$$\alpha = - \left(\frac{1}{d} \right) \ln \left(\frac{T}{(1-R)^2} \right) \quad (4)$$

where T is the transmittance.

Fig. 8 shows the variation of the optical band gap of ZnO:Al films with substrate temperature. As can be seen, the optical band gap increases from 3.41 to 3.64 eV as the substrate temperature increases from 150 to 370 °C. The increase of the band gap with substrate temperature is mainly due to the Burstein–Moss effect [43,44]. In general, the blue shift of the absorption onset of Al doped nanocrystalline films is associated with the increase of the carrier concentration blocking the lowest states in the conduction band, well known as the Burstein–Moss effect [45–46]. This theory predicts that the band gap widening is proportional to $N^{2/3}$. This is in good agreement with electrical measurement showing that carrier concentration of ZnO:Al films increases with substrate temperature.

4. Conclusion

Highly transparent and conductive Al doped zinc oxide thin films have been deposited by DC magnetron sputtering at substrate temperatures ranging between 150 and 370 °C. The films are oriented along the c -axis of the hexagonal structure whatever the substrate temperature. Grain size was found to increase from 10 to 59 nm then decreases to 45 nm as the substrate temperature reaches 370 °C. The optical band gap, carrier concentration and carrier mobility increase with substrate temperature and the highest recorded values are 3.64 eV, $8.6 \times 10^{20} \text{ cm}^{-3}$ and 242 V cm^{-2} , respectively. Deposited ZnO:Al are transparent up to 90% in the visible range. Film resistivity decreases with substrate temperature and a minimum value of $3 \times 10^{-5} \Omega \text{ cm}$ was obtained at 370 °C. The enhancement of electrical properties was attributed to the improvement of crystallinity, surface state and doping effect and the increase of the optical band gap was due to carrier concentration increase. Finally, we can state that substrate temperature is a dominant factor to determine the structural, electrical and optical of ZnO:Al films.

Acknowledgments

The authors gratefully thank Prof. F. Lévy and R. Sanjinès from Institute of Physics of Complex Matter, EPFL, Lausanne, Switzerland for their valuable support.

References

- [1] C.L. Wei, Y.C. Chen, C.C. Cheng, K.S. Kao, D.L. Cheng, P.S. Cheng, *Thin Solid Films* 518 (2010) 3059–3062.
- [2] S. Yodyingyong, Q. Zhang, K. Park, C.S. Dandeneau, X. Zhou, D. Triampo, G. Cao, *Appl. Phys. Lett.* 96 (2010) 73115–73117.
- [3] H. Guo, J. Zhou, Z. Lin, *Electrochem. Commun.* 10 (2008) 146–150.
- [4] D.C. Look, *Mater. Sci. Eng.* 80 (2001) 383–387.
- [5] J.M. Lee, K.K. Kim, S.J. Park, W.K. Choi, *Appl. Phys. Lett.* 78 (2001) 3842–3844.
- [6] H.L. Hartnagel, A.L. Dawar, A.K. Jain, C. Jagadish, *Semiconducting Transparent Thin Films*, Bristol, IOP Publishing, 1995.
- [7] Y.S. Ho, K.Y. Lee, *Thin Solid Films* 519 (2010) 1431–1434.
- [8] C. Zhang, *J. Phys. Chem. Solids* 71 (2010) 364–369.
- [9] K.S. Hwang, B.A. Kang, J.H. Jeong, Y.S. Jeon, B.H. Kim, *Curr. Appl. Phys.* 7 (2007) 421–425.
- [10] E. Bacaksiz, S. Aksu, S. Yilmaz, M. Parlak, M. Altunbaş, *Thin Solid Films* 518 (2010) 4076–4080.
- [11] B.L. Zhu, X.H. Sun, X.Z. Zhao, F.H. Su, G.H. Li, X.G. Wu, J. Wu, R. Wu, J. Liu, *Vacuum* 82 (2008) 495–500.
- [12] Y. Cui, G. Du, Y. Zhang, H. Zhu, B. Zhang, *J. Cryst. Growth* 282 (2005) 389–393.
- [13] K.Y. Tse, H.H. Hong, S.P. Lau, Y.G. Wang, S.F. Yu, *Ceram. Int.* 30 (2004) 1669–1674.
- [14] W.T. Yen, Y.C. Lin, P.C. Yao, J.H. Ke, Y.L. Chen, *Appl. Surf. Sci.* 256 (2010) 3432–3437.
- [15] X. Yu, J. Ma, F. Ji, Y. Wang, X. Zhang, C. Cheng, H. Ma, *Appl. Surf. Sci.* 239 (2005) 222–226.
- [16] J.F. Chang, H.L. Wang, M.H. Hon, *J. Cryst. Growth* 211 (2000) 93–97.
- [17] S.W. Shin, K.U. Sim, J.H. Moon, J.H. Kim, *Curr. Appl. Phys.* 10 (2010) S274–S277.
- [18] S.J. Lim, S. Kwon, H. Kim, *Thin Solid Films* 516 (2008) 1523–1528.
- [19] V. Musat, B. Teixeira, E. Fortunato, R.C.C. Monteiro, P. Vilarinho, *Surf. Coat. Technol.* 180–181 (2004) 659–662.
- [20] X. Zi-qiang, D. Hong, L. Yan, C. Hang, *Mater. Sci. Semicond. Process.* 9 (2006) 132–135.
- [21] S.W. Xue, X.T. Zua, W.G. Zheng, H.X. Deng, X. Xiang, *Physica B* 381 (2006) 209–213.
- [22] H. Ko, W.P. Tai, K.C. Kim, S.H. Kim, S.J. Suh, Y.S. Kim, *J. Cryst. Growth* 277 (2005) 352–358.
- [23] S.S. Lin, J.L. Huang, P. Sajgalik, *Surf. Coat. Technol.* 190 (2005) 39–47.
- [24] E.G. Fu, D.M. Zhuang, G. Zhang, Z. Ming, W.F. Yang, J.J. Liu, *Microelectron. J.* 35 (2004) 383–387.
- [25] F.K. Shan, Y.S. Yu, *J. Eur. Ceram. Soc.* 24 (2004) 1869–1872.
- [26] W. Tang, D.C. Cameron, *Thin Solid Films* 238 (1994) 83–87.
- [27] N. Fujimura, T. Nishihara, S. Goto, J.F. Xu, T. Ito, *J. Cryst. Growth* 130 (1993) 269–279.
- [28] K.H. Kim, R.A. Wibowo, B. Munir, *Mater. Lett.* 60 (2006) 1931–1935.
- [29] J.F. Chang, L. Wang, M.H. Hon, *J. Cryst. Growth* 211 (2000) 93–97.
- [30] E.G. Fu, D.M. Zhuang, G. Zhang, W.F. Yang, M. Zhao, *Appl. Surf. Sci.* 217 (2003) 88–94.
- [31] L. Sagalowicz, G.R. Fox, *J. Mater. Res.* 14 (1999) 1876–1885.
- [32] A. Neiderhofer, P. Nesladek, H.D. Männling, K. Moto, S. Veprek, M. Jille, *Surf. Coat. Technol.* 120–121 (1999) 173–178.
- [33] Q.B. Ma, Z.Z. Ye, H.P. He, J.R. Wang, L.P. Zhu, B.H. Zhao, *Vacuum* 82 (2007) 9–14.
- [34] S.M. Park, T. Ikegami, K. Ebihara, *Thin Solid Films* 513 (2006) 90–94.
- [35] J. Yoo, J. Lee, S. Kim, K. Yoon, I.J. Park, S.K. Dhungel, B. Karunakaran, D. Mangalaraj, J. Yi, *Thin Solid Films* 480–481 (2005) 213–217.
- [36] J.F. Chang, M.H. Hon, *Thin Solid Films* 386 (2001) 79–86.
- [37] Y. Igazaki, H. Saito, *J. Appl. Phys.* 69 (1991) 2190–2195.
- [38] Z.Q. Xu, H. Deng, Y. Li, Q.H. Guo, Y.R. Li, *Mater. Res. Bull.* 41 (2006) 354–358.
- [39] K. Ramamoorthy, K. Kumar, R. Chandramohan, K. Sankaranarayanan, R. Saravanan, I.V. Kityk, P. Ramasamy, *Opt. Commun.* 262 (2006) 91–96.
- [40] F. Chaabouni, M. Abaab, B. Rezig, *Superlattices Microstruct.* 39 (2006) 171–178.
- [41] W.F. Wu, B.S. Chiou, *Thin Solid Films* 298 (1997) 221–227.
- [42] J. Tauc, R. Grigorovichi, A. Vancu, *Phys. Status Solidi B* 15 (1966) 627–637.
- [43] E. Burstein, *Phys. Rev.* 93 (1954) 632–633.
- [44] T.S. Moss, *Proc. Phys. Soc. B* 67 (1954) 775–782.
- [45] E.A. David, N.F. Mott, *Philos. Mag.* 22 (1970) 903–922.
- [46] S.T. Tan, B.J. Chen, X.W. Sun, W.J. Fan, *J. Appl. Phys.* 98 (2005) 013505–013509.